PAN
POLISH ACADEMY OF SCIENCES

Opto-Electronics Review

journal homepage: https://journals.pan.pl/opelre

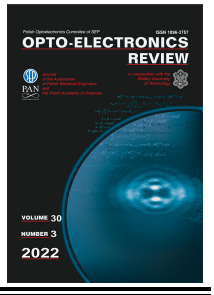

Hybrid PAPR reduction schemes for different OFDM-based VLC systems

Mohamed Y. El-Ganiny[a*], Ashraf A. M. Khalaf[b], Aziza I. Hussein[c], Hesham F. A. Hamed[d]

[a] Department of Electrical Engineering, Higher Technological Institute, 10th of Ramadan City, Sharqia, Egypt
[b] Department of Electrical Engineering, Faculty of Engineering, Minia University, Minia 61519, Egypt
[c] Electrical and Computer Engineering Department, Effat University, Jeddah, Kingdom of Saudi Arabia
[d] Department of Telecommunications Engineering, Egyptian Russian University, Badr City, Egypt

Article info

Article history:
Received 11 Jun. 2022
Received in revised form 13 Jul. 2022
Accepted 20 Jul. 2022
Available on-line 21 Aug. 2022

Keywords:
Visible light communication,
peak-to-average power ratio,
bit error rate.

Abstract

Orthogonal frequency division multiplexing has been widely used in many radio frequency wireless communication standards as a preferable multicarrier modulation scheme. The modulated signals of a conventional orthogonal frequency division multiplexing system are complex and bipolar. In intensity-modulated direct detection optical wireless communications, transmitted signals should be real and unipolar due to non-coherent emissions of an optical light emitting diode. In this paper, different hybrid optical systems have been proposed to satisfy real and unipolar signals. Peak-to-average power ratio is one of the biggest challenges for orthogonal frequency division multiplexing-based visible light communications. They are based on a combination of non-linear companding techniques with spreading or precoding techniques. Simulation evaluation is performed under direct current-biased optical orthogonal frequency division multiplexing, asymmetrically clipped optical orthogonal frequency division multiplexing, and Flip-orthogonal frequency division multiplexing systems in terms of peak-to-average power ratio, bit error rate, and spectral efficiency. The proposed schemes are investigated to determine a scheme with a low peak-to-average power ratio and an acceptable bit error rate. MATLAB^{TM} software has been successfully used to show the validity of the proposed schemes.

1. Introduction

Optical wireless communication (OWC) is considered one of the key technologies to meet the growing demand for high bandwidth and match the requirements to address the congestion problem for the radio frequency (RF) spectrum [1, 2]. OWC led to the birth of a revolutionary communication-based technology called visible light communications (VLC) which uses simple cost-effective devices, and energy-efficient nature-like light emitting diode (LED) at the transmission side and photodiode (PD) at the receiving end [3–5]. The most amazing feature of LED is that it allows simultaneous illumination and communication, which has unlimited applications [1, 3]. This type of communication transmits the signal using an intensity modulation (IM) and receives it using a direct detection (DD) approach. Also, VLC offers unlicensed and huge spectrum compared to RF communications [1–5]. Visible light lies in the range of 400 THz to 700 THz which corresponds to a wavelength of 380 to 780 nm.

VLC technology needs to borrow one of the multicarrier modulation schemes (MCM) such as orthogonal frequency division multiplexing (OFDM) to meet the growing demand for high data rates. Eventually, all these aspects allow VLC communication to be part of the fifth generation (5G) technologies and offer sophisticated services [3, 4, 6].

OFDM-based VLC systems use light signals to modulate the data. The light signals must be real and positive-valued (i.e., unipolar), therefore, a conventional OFDM cannot be implemented without any modifications to its frame structure [1, 4].

*Corresponding author at: mohamed.youssef@hti.edu.eg

https://doi.org/10.24425/opelre.2022.141951
1896-3757/ Association of Polish Electrical Engineers (SEP) and Polish Academic of Sciences (PAS). Published by PAS

Therefore, to accomplish a real and positive-value signal, a variety of optical OFDM versions has been proposed. Each variant of OFDM has its own set of trade-offs in terms of bandwidth/power efficiency, computational complexity, and bit error rate (BER) performance [4, 5].

The most popular optical OFDM systems in the literature are direct current-biased optical OFDM (DCO-OFDM), asymmetrically clipped optical OFDM (ACO-OFDM), and Flip-OFDM. ACO-OFDM and Flip-OFDM can achieve better power consumption than conventional DCO-OFDM at the expense of reducing the bandwidth efficiency [4, 6].

In general, all optical OFDM systems mentioned suffer from a significant peak-to-average power ratio (PAPR) challenge and the need for a high-power amplifier at the transmission side. PAPR reduction techniques can be classified into three main groups based on their strategy: coding, signal distortion, and probabilistic approaches [7, 8].

The main purpose of this work is to investigate hybrid PAPR schemes and compare their performance via different MCM VLC-based systems (i.e., DCO-OFDM, ACO-OFDM, and Flip-OFDM) which have different spectral efficiency (as derived in section 2).

Hence, the major focus of this work is to present an elaborate discussion on some probabilistic PAPR reduction techniques. Also, two hybrid PAPR reduction schemes are introduced. The first hybrid structure is based on a combination of precoding techniques with non-linear companding PAPR reduction approaches. The second one is a combination of spreading techniques with non-linear companding PAPR reduction approaches. Finally, an optimum hybrid scheme with a suitable MCM-based VLC system as the preferred structure for 5G technology is identified.

The rest of the paper is organized as follows: in section 2, a concise description of several OFDM-based VLC systems is presented. Section 3 describes the PAPR reduction techniques. The proposed hybrid PAPR system is presented in section 4. The simulation results for the proposed hybrid PAPR scheme and a comparison with the conventional schemes are presented in section 5. Finally, the conclusion is drawn in section 6.

2. OFDM-based VLC systems

This section is directed toward a brief discussion of different MCM formats that are more adaptable to be used for IM/DD-based VLC systems. Here, DCO-OFDM, ACO-OFDM, and Flip-OFDM multicarrier modulation formats will be investigated. A brief characteristics of each will be presented in the following sections below. The most common point for those is the methodology used to make the conventional OFDM signals real and positive-valued.

2.1. DCO-OFDM

DCO-OFDM is considered as one of the simplest and earliest MCM techniques to be compatible with IM/DD systems by generating a real and non-negative-valued OFDM scheme. It involves adding DC-bias to the signal which is supposed to be in unipolar format [9, 10]. The block diagram of DCO-OFDM is shown in Fig. 1.

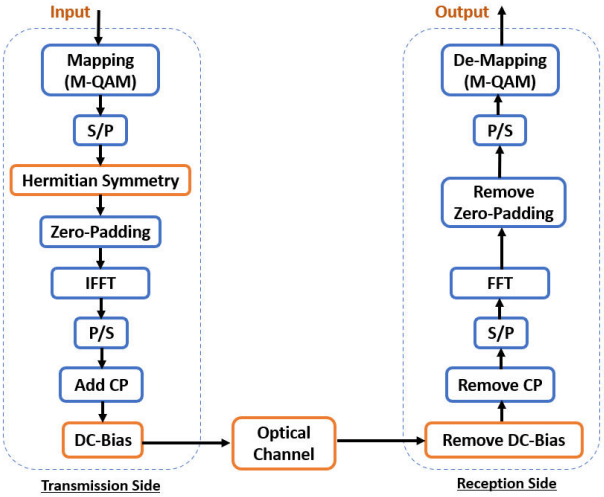

Fig. 1. DCO-OFDM system model.

As depicted from the figure, the incoming data stream is being mapped into M-QAM symbols where M signifies the constellation order. Further, these high-speed symbols are split into low-speed data sets using a serial to parallel (S/P) converter [11, 12].

In DCO-OFDM, Hermitian symmetry (HS) with inverse fast Fourier transform (IFFT) are used to convert the complex-valued to real as shown in Fig. 2.

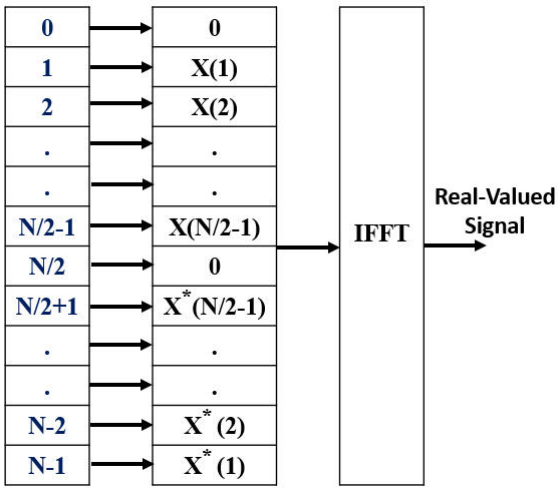

Fig. 2. Hermitian symmetry imposed IFFT.

Due to the HS constraint, the spectral efficiency is reduced and only the first half of subcarriers is used to carry data while the remaining subcarriers are flipped complex conjugates of the first half (i.e., out of IFFT size of N, only N/2 carry data). Mathematically, the operation of HS can be represented as

$$X[N-k] = X^*[k], k = 1,2,\ldots.\frac{N}{2}. \quad (1)$$

To avoid the imaginary part at the IFFT output, the first $X[0]$ and the middle $X\left[\frac{N}{2}\right]$ subcarriers are set to be zero.

$$X[0] = X\left[\frac{N}{2}\right] = 0. \quad (2)$$

The input to the IFFT has the following representation:

$$X = [0, X_1, X_2, .. X_{\frac{N}{2}-1}, 0, X^*_{\frac{N}{2}-1}, .., X_2{}^*, X_1{}^*]^T. \quad (3)$$

To avoid the effect of inter-symbol interference (ISI), a certain amount of cyclic prefix (CP) is inserted to the output of IFFT after a parallel-to-serial (P/S) converter [13, 14]. Finally, a pre-defined value of DC-bias is added to attain a positive-valued signal. After the optical signal is transmitted through the optical channel, inverse operations are performed for all these blocks to retrieve the original data.

2.2. ACO-OFDM

ACO-OFDM approach can be used to reach a positive-valued signal and overcome the disadvantage of DCO-OFDM in terms of power efficiency at the expense of decreasing bandwidth efficiency. Consequently, a unipolar signal can be generated without the need for DC-bias. In ACO-OFDM, only odd subcarriers are used, but the even subcarriers are set to zero. Hence, only N/4 subcarriers are used due to the HS constraint and only half subcarriers are involved in data transmission (i.e., noise due to clipping falls only on even subcarriers) [15].

ACO-OFDM system model is shown in Fig. 3. It is shown that this model performs mapping of odd subcarriers before HS. Also, instead of DC-bias block in DCO-OFDM, ACO-OFDM system model has zero-clipping block to reach the positive-valued signal and clip the negative part.

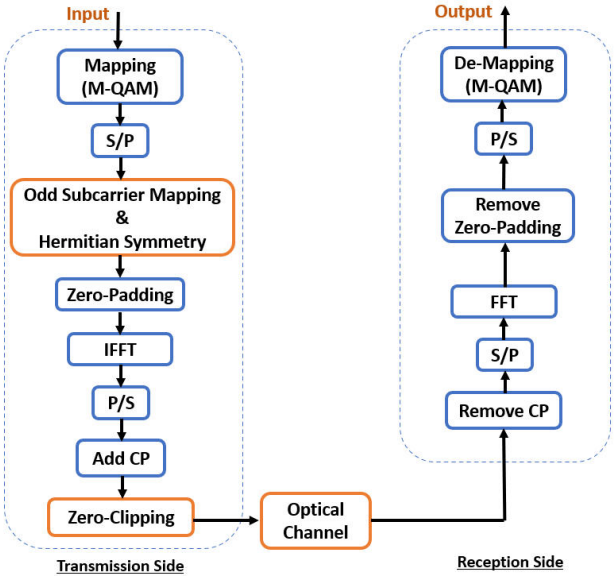

Fig. 3. ACO-OFDM system model.

2.3. Flip-OFDM

This is an alternative optical OFDM scheme that meets the IM/DD systems requirements which need the signal to be real and unipolar [16, 17]. Here, only half of the subcarriers are used. As shown in Fig. 4, Flip-OFDM system uses the HS criteria to fetch the signal in real format. However, without the need for biasing like DCO-OFDM or zero-clipping like ACO-OFDM, Flip-OFDM converts the bipolar signal into unipolar.

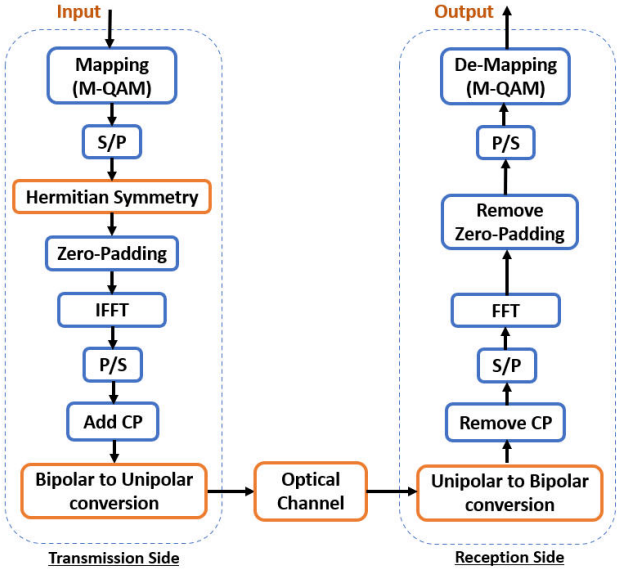

Fig. 4. Flip-OFDM system model.

This conversion is performed by isolating the positive-valued components from the negative-valued components, flipping the negative part and then transmitting both positive and flipped negative parts in two consecutive frames as shown in Fig. 5 [16].

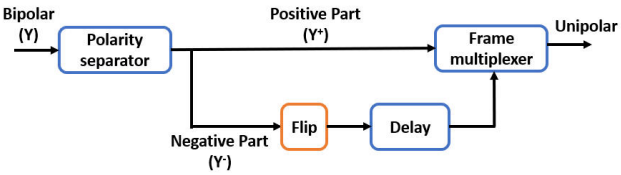

Fig. 5. Bipolar to unipolar conversion.

2.4. Comparison between DCO-OFDM, ACO-OFDM, and Flip-OFDM

2.4.1. Spectral efficiency comparison

The spectral efficiency of DCO-OFDM is reduced to half when compared to the conventional OFDM system due to the usage of HS. On the other hand, the spectral efficiency of ACO-OFDM and Flip-OFDM is reduced to half when compared with DCO-OFDM (i.e., reduced to ¼ when compared with a conventional OFDM), due to the fact that only odd subcarriers can be used for ACO-OFDM data transmission and due to the bipolar to unipolar conversion block for the Flip-OFDM scheme [17]. Consequently, the achievable spectral efficiency of DCO-OFDM can be expressed by (4)

$$\eta_{DCO} = \frac{\log_2 M\,(N_{FFT} - 2)}{2(N_{FFT} + N_{CP})} \text{ bits/s/Hz.} \quad (4)$$

On the other hand, the spectral efficiency of both ACO-OFDM and Flip-OFDM can be represented by (5)

$$\eta_{ACO\ \&\ Flip} = \frac{\log_2 M\,(N_{FFT} - 2)}{4(N_{FFT} + N_{CP})} \text{ bits/s/Hz.} \quad (5)$$

The parameter $\log_2 M$ indicates the total number of bits for each QAM symbol, N_{FFT} represents the IFFT/FFT size, N_{CP} is the cyclic prefix length, while $(N_{FFT}-2)/2$ indicates that the first and middle subcarriers are set to zero due to the HS criteria.

Using (4) and (5), Figure 6 depicts the spectral efficiency for DCO-OFDM, ACO-OFDM, and Flip-OFDM. The simulation results show that the DCO-OFDM system has higher spectral efficiency than ACO-OFDM and Flip-OFDM. The spectral efficiency has been evaluated by 4QAM symbols [i.e., modulation order $(M) = 4$] and a cyclic prefix length of 256.

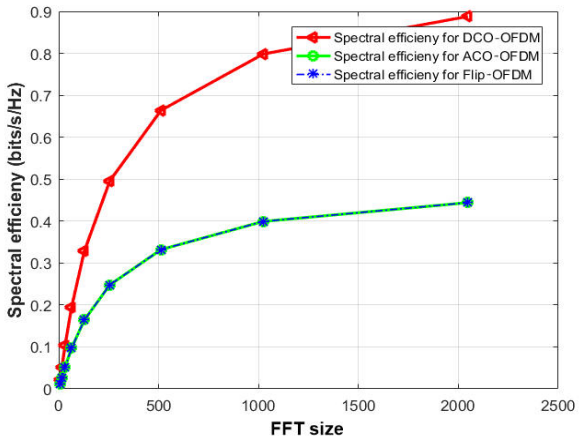

Fig. 6. Spectral efficiency for DCO-OFDM, ACO-OFDM, and Flip-OFDM.

2.4.2. Computational complexity comparison

The term of computational complexity refers to the number of operations for both IFFT at transmitter and FFT at receiver. Here, the computational complexity for DCO-OFDM, ACO-OFDM, and Flip-OFDM is given in Table 1.

Table 1.
Complexity comparison of DCO-OFDM, ACO-OFDM, and Flip-OFDM.

Optical OFDM System	Complexity	
	Transmitter	Receiver
DCO-OFDM	$N\log(N)$	$N\log(N)$
ACO-OFDM	$2(N/2)\log(N/2)$	$2N\log(N)$
Flip-OFDM	$N\log(N)$	$N\log(N)$

It is shown that at the transmission side both DCO-OFDM and Flip-OFDM have the same complexity while they are nearly the same when compared with ACO-OFDM for a significant number of IFFT/FFT size (N). However, at the reception side, Flip-OFDM and DCO-OFDM optical systems reduce the hardware complexity by 50% because compared to ACO-OFDM, they provide a transformation of twice as much data information [16].

3. PAPR reduction techniques

Optical OFDM systems are the most popular MCM scheme meeting the requirements for VLC communication systems in terms of high data rate. On the other hand, it suffers from high PAPR due to a huge number of subcarriers [18, 19]. The PAPR of optical OFDM signals is given by

$$\mathrm{PAPR} = 10\log_{10}\left[\frac{Max\left(\left|y_{\mathrm{unipolar}}\right|^2\right)}{E\left(\left|y_{\mathrm{unipolar}}\right|^2\right)}\right], \tag{6}$$

where $E(.)$ stands for the expectation operator. A complementary cumulative distribution function (CCDF) used to evaluate the probability that PAPR of an optical OFDM symbol exceeds a certain threshold (PAPR_0) which is expressed by

$$\mathrm{CCDF} = Pr(\mathrm{PAPR} > \mathrm{PAPR}_0). \tag{7}$$

Consequently, it is vital to investigate the PAPR reduction approaches. From the literature (i.e., as shown in Fig. 7), PAPR reduction techniques can be classified into three different approaches: coding, signal distortion, and probabilistic approaches [20, 21]. Each reduction approach has its own set of advantages and disadvantages. One of those is chosen according to a desired performance for the system. The performance here is evaluated in terms of reduction capabilities in a confrontation of BER performance, in-band and out-of-band distortion, reduction in the data rate, and computational complexity. The coding approach tends to select the best codeword that minimizes PAPR, but it decreases the spectral efficiency because it adds extra bits which will also decrease the data rate. Block coding, Golay sequence, and Reed-Muller code can be used in this approach. Signal distortion approach limits the signal amplitude to a pre-defined level which causes in-band and out-of-band distortion. Clipping and filtering technique is considered the easiest technique to determine the value of PAPR while it comes against the BER performance. Peak windowing decreases the peaks of the signal that are above a particular threshold, which is performed by using one of the window functions (i.e., kaiser or Hamming window). Peak windowing technique has a lower spectral growth. Therefore, it has attenuated the out-of-band emission compared to the clipping technique. On the other hand, the companding technique is used to compress the signal which has a high dynamic range to process it in a sufficient strategy with a low dynamic range.

Finally, it limits the overall signal range which reduces the value of PAPR. The BER performance of this technique depends on a pre-defined value of the companding factor. Meanwhile, the probabilistic approach tends to minimize the likelihood of a high PAPR [22, 23]. Selected mapping technique (SLM) and partial transmit sequence (PTS) are effective and distortion-free strategies that can be used for PAPR reduction. One sequence must be selected which has a lower PAPR by introducing a random phase rotation. However, these techniques decrease the spectral efficiency

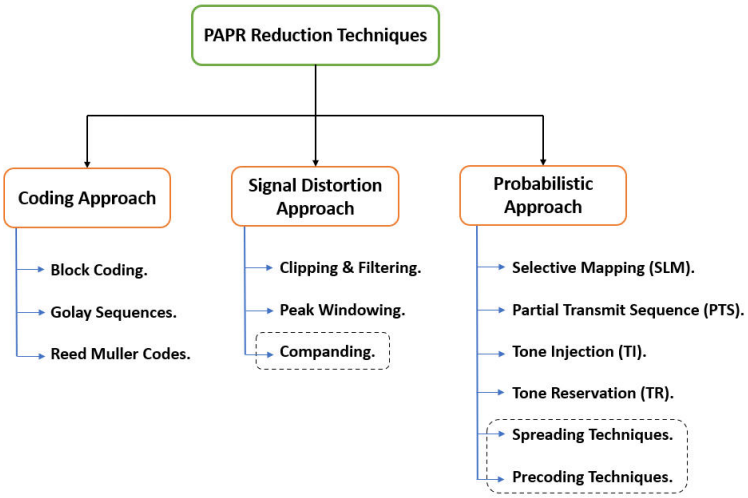

Fig. 7. PAPR reduction techniques.

due to the side information that must be transmitted with the original information to help the receiver to attain the original data. For PTS technique, this phase rotation is applied to each subcarrier, but the phase rotation is applied to all subcarriers in case of the SLM technique. Consequently, the computational complexity for PTS is higher than for SLM. Also, tone injection and tone reservation strategies decrease the spectral efficiency and the overall data rate. The precoding and spreading techniques will be illustrated in section 3.1 and 3.2, respectively.

Also, a hybrid approach can be performed from the available PAPR reduction techniques. In this paper, a hybrid PAPR reduction scheme between a non-linear companding and different precoding techniques is investigated. Also, a combination of non-linear companding and spreading techniques is performed. All these schemes are performed and evaluated through DCO-OFDM, ACO-OFDM, and Flip-OFDM optical systems.

3.1. Precoding techniques

Precoding technique is considered one of the vital approaches to minimize the PAPR value by reducing the autocorrelation of the input sequence [24, 25]. Here, some precoding techniques under DCO-OFDM, ACO-OFDM, and Flip-OFDM optical systems are evaluated. For all these systems, precoding block is performed before IFFT procedure. The system model of applying the precoding approach under DCO-OFDM, ACO-OFDM, and Flip-OFDM optical systems is shown in Fig. 8.

At the transmission side, the precoding block is performed after mapping the input data sequence in complex format and serial-to-parallel converter [26, 27]. The output of the precoding block can follow different paths for DCO-OFDM, ACO-OFDM, and Flip-OFDM systems. The HS block is performed for DCO-OFDM and Flip-OFDM paths. For ACO-OFDM, an odd subcarrier mapping (OSM) block is performed before an HS block. Finally, the selection between DC-bias for DCO-OFDM or zero-clipping for ACO-OFDM, or bipolar to unipolar conversion (B/U) for Flip-OFDM is performed after zero-padding, IFFT, and CP insertion blocks. At the reception side, the DC-bias is removed for DCO-OFDM or unipolar

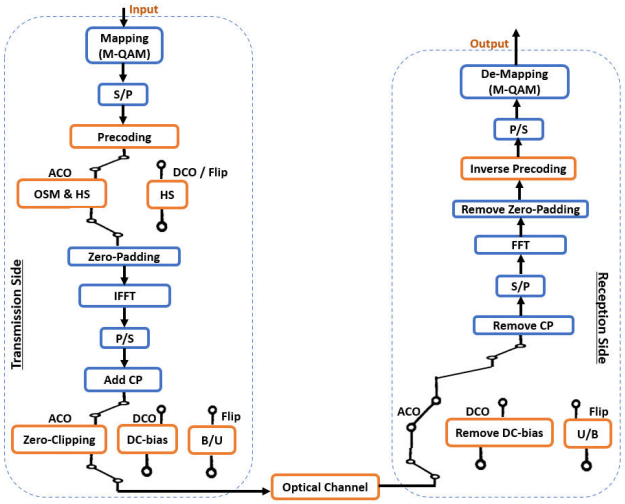

Fig. 8. Illustration of the use of precoding techniques in various optical OFDM systems.

to bipolar conversion (U/B) block is used to retrieve the bipolar signal for Flip-OFDM system. The inverse precoding approach is performed after CP removal, FFT, and zero-padding removal. Finally, the data sequence is retrieved using a de-mapper block.

Here, precoding techniques such as discrete cosine transform (DCT), discrete sine transform (DST), discrete Hartley transform (DHT), and discrete Fourier transform (DFT) are investigated.

3.1.1. Discrete cosine transform (DCT)

The DCT transformation involves the multiplication between the data input and the cosine equation. Each element of the DCT matrix B of size $N \times N$ in the m-th row and n-th column is given by [12, 14]

$$B_{m,n} = \begin{cases} \frac{1}{\sqrt{N}}\left[\cos\left(\frac{\pi}{N}(n+0.5)m\right)\right], & 1 \le m \le N-1, \\ & 0 \le n \le N-1, \\ \frac{1}{\sqrt{N}}, & m = 0, \\ & 0 \le n \le N-1. \end{cases} \quad (8)$$

3.1.2 Discrete sine transform (DST)

Here, the multiplication is performed with a sine equation. Each element of the DST matrix B of size $N \times N$ in the m-th row and n-th column is defined as follows [18]:

$$B_{m,n} = \sqrt{\frac{2}{N}} \cdot \gamma \cdot \left[\sin\left(\frac{\pi(2m+1)(n+1)}{2N}\right) \right], \quad (9)$$

where

$$0 \le m \le N-1,\ 0 \le n \le N-1, \text{ and } \gamma = \begin{cases} \frac{1}{\sqrt{2}}, & m = N-1 \\ 1, & \text{o.w} \end{cases}$$

3.1.3. Discrete Hartley transform (DHT)

It is a real trigonometric transform with a self-inverse property. The output sequence of a DHT precoding technique is performed by multiplication between the input data sequence and the following equation [28, 29]. Each element of DHT matrix B of size $N \times N$ in the m-th row and n-th column is defined as follows:

$$B_{m,n} = \frac{1}{\sqrt{N}} \left[\cos\left(\frac{2\pi}{N} mn\right) + \sin\left(\frac{2\pi}{N} mn\right) \right], \quad (10)$$

where $m \ge 0,\ n \le N-1$.

3.1.4. Discrete Fourier transform (DFT)

The DFT precoding block, like all precoding techniques, adds an extra computational complexity to the system when compared with the conventional optical system [30, 31].

Each element of DFT matrix B of size $N \times N$ in the m-th row and n-th column is defined as follows:

$$B_{m,n} = \exp\left(j\frac{2\pi mn}{N}\right), \quad (11)$$

where $m \ge 0,\ n \le N-1$.

3.2. Spreading techniques

Spreading approach is considered an effective way to reduce the PAPR of the optical signals. This approach improves the BER performance of the conventional optical systems as shown later. Here, different spreading techniques such as DCT-spreading, DST-spreading, DHT-spreading, and DFT-spreading are investigated. In the transmitter, this approach is implemented by forcing the M-point DCT/DST/DHT/DFT-spreading before the N-point IFFT operation to represent the transmitted data in the frequency domain [31, 32].

As can be seen in Fig. 9, a set of data symbols is mapped using M-QAM and transmitted in parallel, and then the spreading phenomenon is applied. The subcarrier mapping technique is applied to the output of DCT/DST/DHT/DFT-spreading. Other blocks of this system follow the same methodology of the system shown previously in Fig. 8. Finally, the inverse operation of the spreading technique is performed at the reception side.

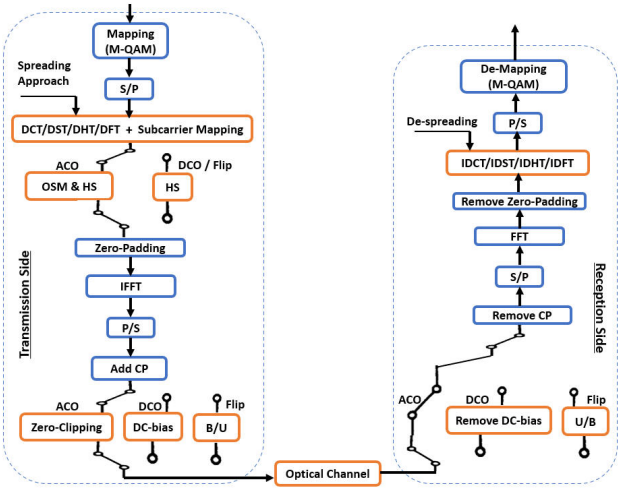

Fig. 9. Use of the spreading approach in optical OFDM systems.

Figure 10 represents the subcarrier mapping using 8-point DCT/DST/DHT/DFT and 16-point IFFT.

3.3. Non-linear companding techniques

Companding techniques are a noteworthy approach that can be used to diminish the PAPR level. Optical signals are compressed at the transmission side and reconstructed again at the reception side. Here, μ-law and A-law companding techniques are introduced [33].

3.3.1. μ-law companding

For a given signal x, the output of the μ-law compressor is

$$y(x) = V_{max} \frac{\log\left(1 + \frac{\mu|x|}{V_{max}}\right)}{\log(1+\mu)} \operatorname{sgn}(x), \quad (12)$$

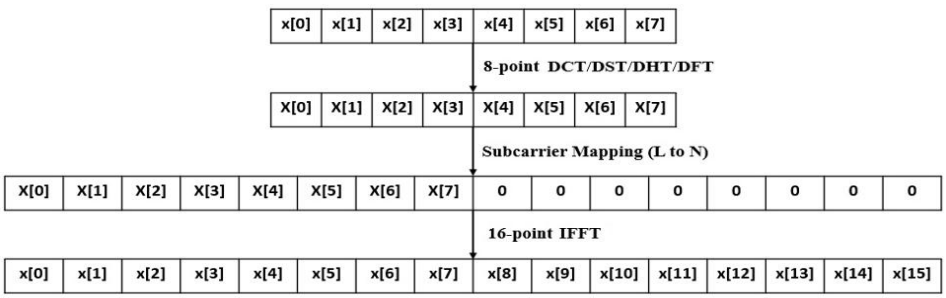

Fig. 10. Signal format depicting the optical OFDM mapping strategy.

where V_{max} is the maximum value of the signal x, μ is the μ-law parameter of the compander, log is the natural logarithm and sgn is the signum function.

3.3.2. *A-law companding*

The output of the A-law compressor is

$$y(x) = \begin{cases} \dfrac{A|x|}{1+\log A}\,\mathrm{sgn}(x), & 0 \le |x| \le \dfrac{V_{max}}{A} \\ V_{max}\,\dfrac{1+\log\left(\dfrac{A|x|}{V_{max}}\right)}{1+\log A}\,\mathrm{sgn}(x), & \dfrac{V_{max}}{A} < |x| \le V_{max}. \end{cases} \quad (13)$$

4. Proposed hybrid PAPR reduction scheme

As mentioned before in the literature, one of the major constraints for the optical systems is that the modulated signals should be real and unipolar. Consequently, different approaches are investigated in this direction to fit these considerations. Also, many studies are performed to reduce the PAPR level and take into account the BER performance and the computational complexity. Figure 11 represents the proposed hybrid scheme that has been nominated by authors to minimize the PAPR level for optical signals.

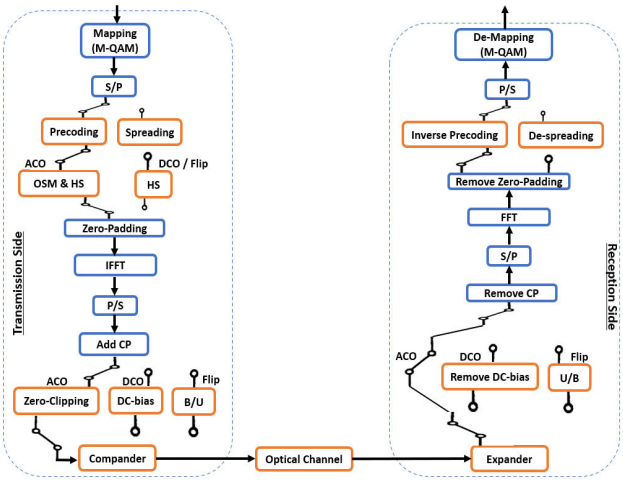

Fig. 11 Proposed optical system with hybrid precoding/ spreading and companding of PAPR reduction schemes.

The proposed scheme is based on combining the precoding or spreading techniques with the non-linear companding techniques. The performance is evaluated under DCO-OFDM, ACO-OFDM, and Flip-OFDM optical systems in terms of PAPR calculation and BER performance. These optical systems were previously illustrated in sections 2.1, 2.2, and 2.3, respectively. A brief description and a mathematical model for the precoding and spreading techniques were also previously discussed in sections 3.1 and 3.2, respectively while the non-linear companding techniques were previously introduced in section 3.3.

The simulation parameters of the optical systems are shown in Table 2.

Table 2.
Optical systems parameters.

Parameter	Value
FFT and IFFT size (N)	1024
Number of subcarriers (L)	800
Zero-padding	2 × 112
Mapping	M-QAM
Modulation order (M)	4
Cyclic prefix length (N_{cp})	256

5. Simulation results

This section shows the performance analysis of hybrid PAPR reduction schemes under different optical OFDM systems. The BER performance and PAPR calculations of the suggested PAPR reduction techniques are evaluated.

The efficiency of the proposed scheme-based optical OFDM system is shown by comparing the results with the conventional DCO-OFDM, ACO-OFDM, and Flip-OFDM results. For this comparison purposes, the values of $PAPR_0$ of the proposed schemes are compared with the values of $PAPR_0$ for the conventional systems at CCDF = 10^{-2} and the required value E_b/N_0 at BER = 10^{-3}.

The results show that the values of $PAPR_0$ of conventional DCO-OFDM, ACO-OFDM, and Flip-OFDM are 15.72 dB, 16.10 dB, and 15.90 dB, respectively at CCDF = 10^{-2}. Also, the values of the required E_b/N_0 for these conventional systems are 11.82 dB, 6.40 dB, and 6.80 dB, respectively at BER = 10^{-3}.

5.1. *DCO-OFDM*

5.1.1. *PAPR and BER performance for precoding techniques*

This section shows PAPR and BER performance for DCT, DST, DHT, and DFT precoding techniques under DCO-OFDM system. As shown in Fig. 12, at CCDF = 10^{-2}, DCT and DST precoding techniques reduce the PAPR to a value close to 13 dB. Also, the PAPR value of DHT precoding technique is nearly of 13.8 dB. Consequently, the PAPR reduction values are 2.72, 2.72, and 1.92 dB for DCT, DST, and DHT, respectively when compared to the conventional DCO-OFDM system. The PAPR value of DFT precoding technique is almost the same value for the conventional DCO-OFDM.

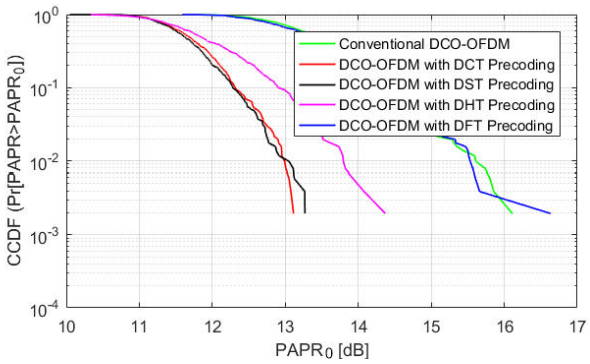

Fig. 12. PAPR comparison between DCT, DST, DHT, and DFT precoding techniques for DCO-OFDM system.

On the other hand, the BER performance for all these precoding techniques is almost the same performance when compared to the conventional DCO-OFDM as shown in Fig. 13.

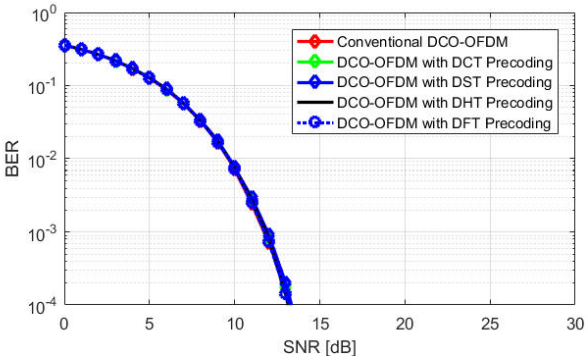

Fig. 13. BER comparison between DCT, DST, DHT, and DFT precoding techniques for DCO-OFDM system.

5.1.2. *PAPR and BER performance for precoding techniques combined with μ-law companding*

Figures 14 and 15 show the PAPR and BER performance, respectively for the precoding techniques when combined with μ-law companding under DCO-OFDM system with the companding factor (μ) equalling 3. The value of $PAPR_0$ at CCDF = 10^{-2} equals 10.14, 10.04, 10.74, and 12.07 dB for DCT, DST, DHT, and DFT combined with μ-law companding, respectively. Consequently, the PAPR reduction value when compared to the conventional DCO-OFDM system equals 5.58, 5.68, 4.98, and 3.65 dB for the combination between μ-law companding and DCT, DST, DHT, and DFT, respectively. Also, this approach is evaluated with different companding factor (μ) = 2, 3, and 5 and the results shown finally in Table A1.

On the other hand, the BER performance is almost the same performance for DCT, DST, and DHT when compared to the conventional DCO-OFDM as shown in Fig. 15. For DFT precoding combined with μ-law companding, the required E_b/N_0 is 30 dB to achieve BER = 10^{-3} which means that the required E_b/N_0 is increased by 18.18 dB when compared with the conventional DCO-OFDM system.

5.1.3. *PAPR and BER performance for precoding techniques combined with A-law companding*

Figures 16 and 17 show the PAPR and BER performance, respectively for the precoding techniques when combined with A-law companding under DCO-OFDM system with a companding factor (A) equalling 3. The value of $PAPR_0$ at CCDF = 10^{-2} equals 10.40, 10.40, 11.43, and 13.25 dB for DCT, DST, DHT, and DFT combined with A-law companding, respectively. Consequently, the PAPR reduction value when compared to the conventional DCO-OFDM system equals 5.32, 5.32, 4.29, and 2.47 dB for the combination between A-law companding and DCT, DST, DHT, and DFT, respectively. Also, this approach is evaluated with a different companding factor (A) = 2, 3, and 5 and the results are shown finally in Table A1.

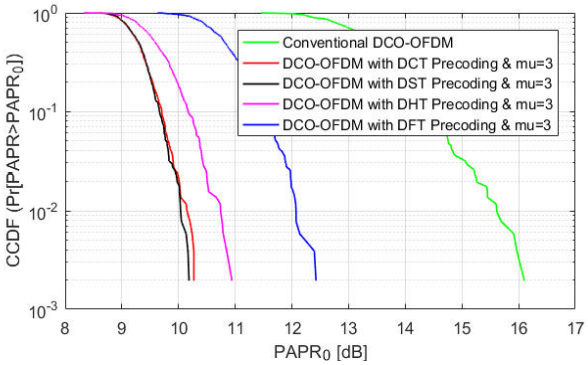

Fig. 14. PAPR comparison between precoding techniques combined with μ-law companding for DCO-OFDM system.

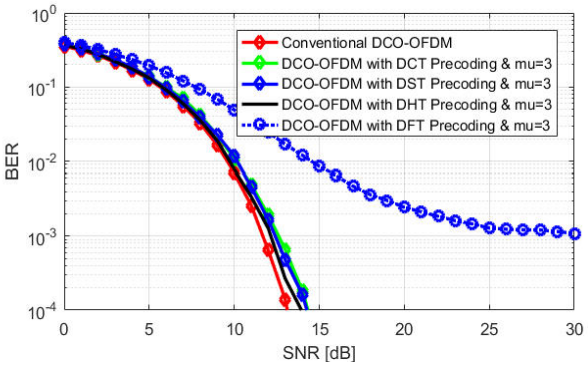

Fig. 15. BER comparison between precoding techniques combined with μ-law companding for DCO-OFDM system.

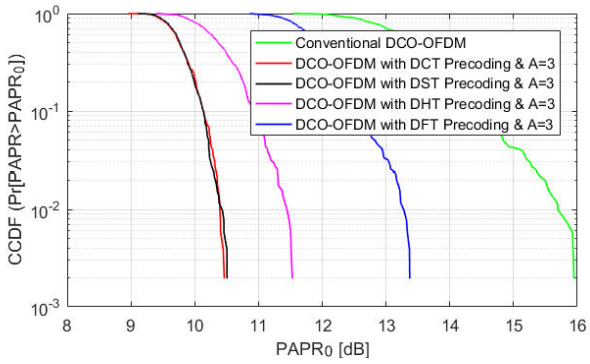

Fig. 16. PAPR comparison between precoding techniques combined with A-law companding for DCO-OFDM system.

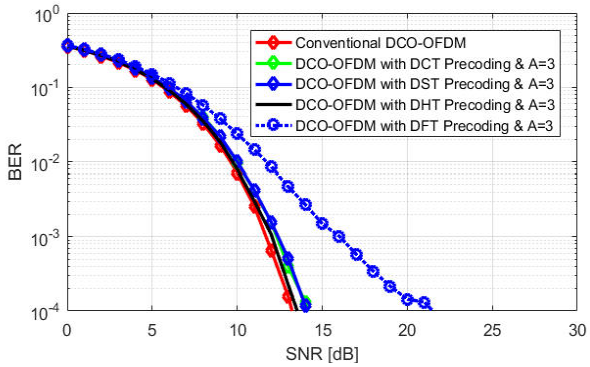

Fig. 17. BER comparison between precoding techniques combined with A-law companding for DCO-OFDM system.

On the other hand, the BER performance is almost the same performance for DCT, DST, and DHT when compared to the conventional DCO-OFDM as shown in Fig. 17. For DFT precoding combined with A-law companding, the required E_b/N_0 is 16 dB to achieve BER = 10^{-3} which means that the required E_b/N_0 is increased by 4.18 dB when compared with the conventional DCO-OFDM system.

5.1.4. *PAPR and BER performance for spreading techniques*

This section also shows the results of PAPR and BER performance for DCT, DST, DFT, and DHT-spreading techniques under DCO-OFDM system. As shown in Fig. 18, at CCDF = 10^{-2}, spreading techniques of DCT and DST reduce the PAPR to a value of nearly 12.95 and 12.89 dB, respectively. Also, the PAPR value of DHT-spreading technique is nearly of 13.78 dB. On the other hand, the value of $PAPR_0$ of DFT-spreading technique is 12.15 dB. Consequently, the PAPR reduction value is 2.77, 2.83, 1.94, and 3.57 dB for DCT, DST, DHT, and DFT, respectively when compared to the conventional DCO-OFDM system.

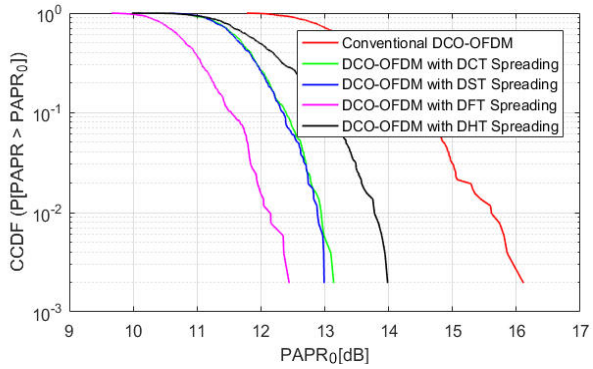

Fig. 18. PAPR comparison between DCT, DST, DHT, and DFT spreading techniques for DCO-OFDM system.

On the other hand, the BER performance for all these spreading techniques is almost the same and the value of E_b/N_0 is 8.8 dB at BER = 10^{-3} which means that the spreading techniques have a gain of 3.02 dB compared to the conventional DCO-OFDM as shown in Fig. 19.

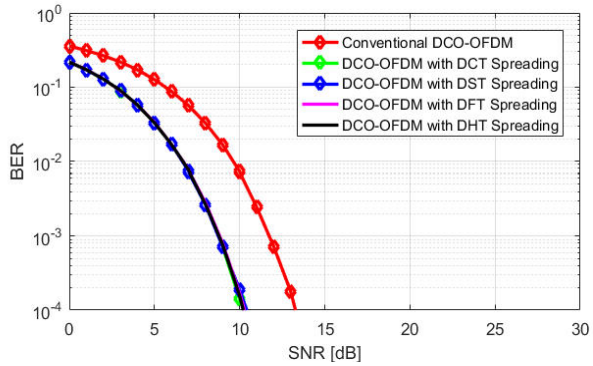

Fig. 19. BER comparison between DCT, DST, DHT, and DFT spreading techniques for DCO-OFDM system.

5.1.5. *PAPR and BER performance for spreading techniques combined with μ-law companding*

DCT, DST, DFT, and DHT-spreading techniques combined with μ-law companding under DCO-OFDM system are presented in this section. As shown in Fig. 20, at CCDF = 10^{-2}, spreading techniques of DCT, DST, DHT, and DFT combined with μ-law companding reduce the PAPR to a value of nearly 10.05, 10.05, 11.64, and 9.30 dB, respectively. Consequently, the PAPR reduction value is 5.67, 5.67, 4.08, and 6.42 dB for DCT, DST, DHT, and DFT, respectively when compared to the conventional DCO-OFDM system.

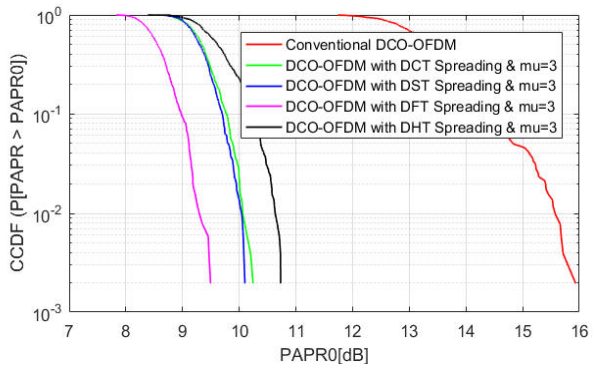

Fig. 20. PAPR comparison between spreading techniques combi-ned with μ-law companding for DCO-OFDM system.

On the other hand, BER performance for DCT, DST, DHT, and DFT-spreading techniques combined with μ-law companding to achieve BER = 10^{-3} need E_b/N_0 equalling 9.5, 9.5, 9.15, and 9.07 dB, respectively which means that the required E_b/N_0 is decreased by 2.32, 2.32, 2.67, and 2.12 dB for DCT, DST, DHT, and DFT-spreading techniques combined with μ-law companding when compared with the conventional DCO-OFDM system as shown in Fig. 21.

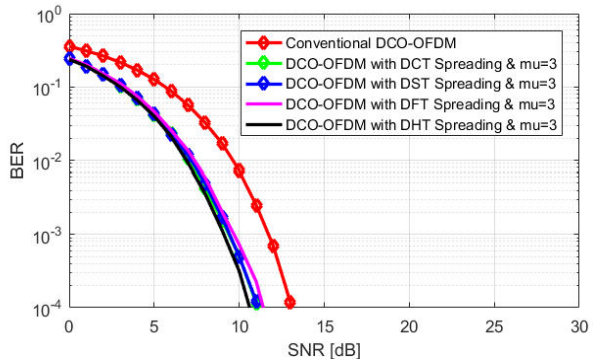

Fig. 21. BER comparison between spreading techniques combined with μ-law companding for DCO-OFDM system.

5.1.6. *PAPR and BER performance for spreading techniques combined with A-law companding.*

The combination between these spreading techniques and A-law companding under DCO-OFDM system is presented in this section. As shown in Fig. 22, at CCDF = 10^{-2}, spreading techniques of DCT, DST, DHT,

and DFT combined with A-law companding reduce the PAPR to a value of nearly 10.65, 10.56, 11.23, and 9.82 dB, respectively. Consequently, the PAPR reduction value is 5.07, 5.16, 4.49, and 5.9 dB for DCT, DST, DHT, and DFT, respectively when compared to the conventional DCO-OFDM system.

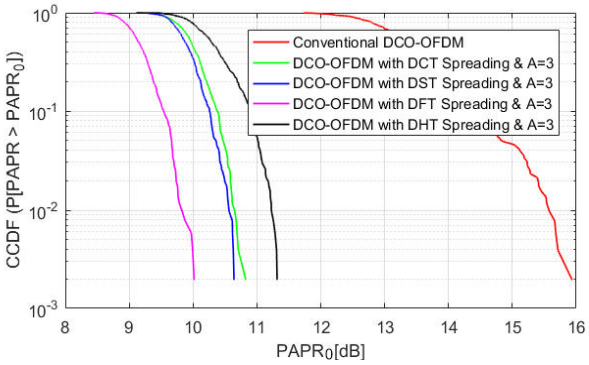

Fig. 22. PAPR comparison between spreading techniques combined with A-law companding for DCO-OFDM system.

On the other hand, BER performance for DCT, DST, DHT, and DFT-spreading techniques combined with A-law companding to achieve BER = 10^{-3} need E_b/N_0 equalling 9, 9.2, 8.91, and 9.10 dB which means that the required E_b/N_0 is reduced by 2.82, 2.62, 2.91, and 2.72 dB for DCT, DST, DHT, and DFT-spreading techniques combined with A-law companding when compared with the conventional DCO-OFDM system as shown in Fig. 23.

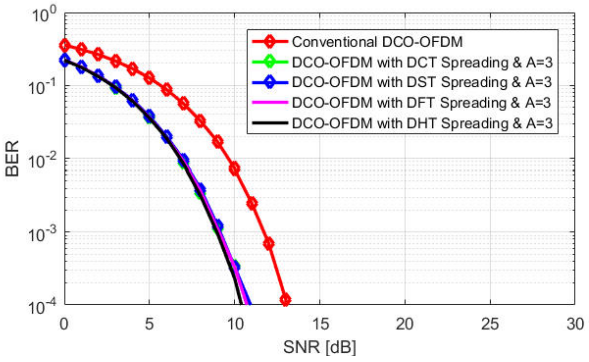

Fig. 23. BER comparison between spreading techniques combined with A-law companding for DCO-OFDM system.

5.2. *ACO-OFDM*

5.2.1. *PAPR and BER performance for precoding techniques*

This section shows the PAPR and BER performance for DCT, DST, DHT, and DFT precoding techniques under ACO-OFDM system. As shown in Fig. 24, at CCDF = 10^{-2}, precoding techniques of DCT, DST, DHT, and DFT reduce the PAPR to a value of nearly 11.86, 13.20, 14.10, and 16.25 dB, respectively. Consequently, the PAPR reduction value is 4.24, 2.9, 2, and 0.15 dB for DCT, DST, DHT, and DFT, respectively when compared to the conventional ACO-OFDM system.

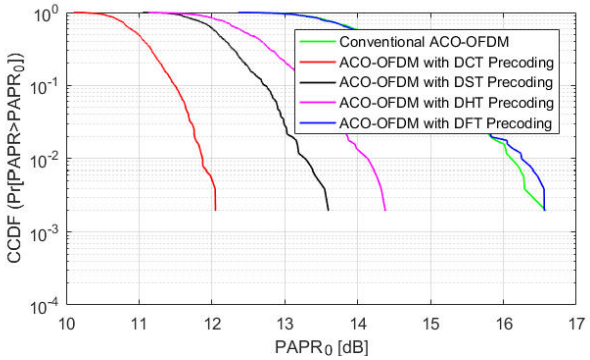

Fig. 24. PAPR comparison between DCT, DST, DHT, and DFT precoding techniques for ACO-OFDM system

On the other hand, the BER performance for all these precoding techniques is almost the same performance when compared to the conventional ACO-OFDM as shown in Fig. 25.

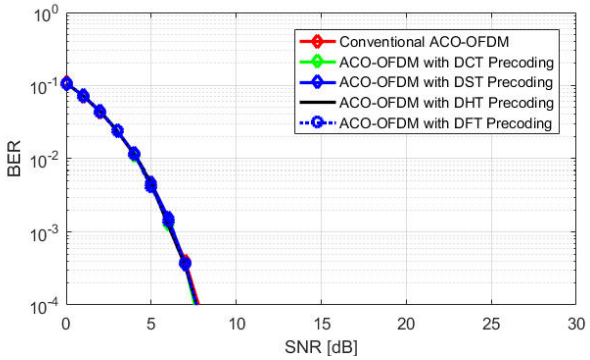

Fig. 25. BER comparison between DCT, DST, DHT, and DFT precoding techniques for ACO-OFDM system.

5.2.2. *PAPR and BER performance for precoding techniques combined with μ-law companding*

Figures 26 and 27 show the PAPR and BER performance, respectively for the precoding techniques when combined with μ-law companding under ACO-OFDM system with the companding factor (μ) equalling 3. The value of $PAPR_0$ at CCDF = 10^{-2} equals 9.44, 10.46, 11.06, and 12.93 dB for DCT, DST, DHT, and DFT combined with μ-law companding, respectively.

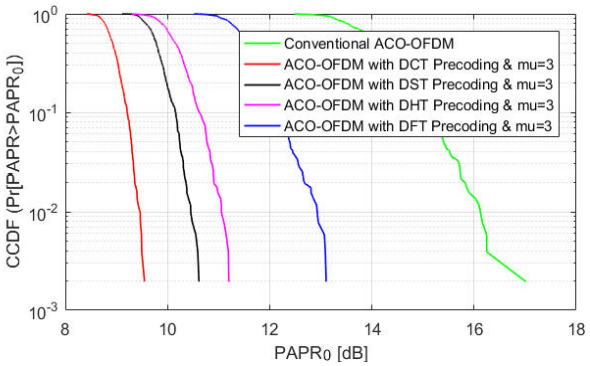

Fig. 26. PAPR comparison between precoding techniques combined with μ-law companding for ACO-OFDM system.

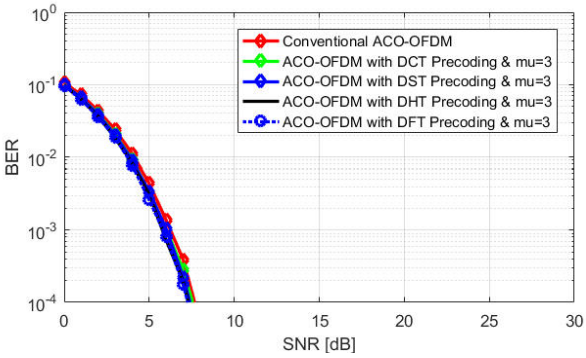

Fig. 27. BER comparison between precoding techniques combined with μ-law companding for ACO-OFDM system.

Consequently, the PAPR reduction value when compared to the conventional ACO-OFDM system is 6.66, 5.64, 5.04, and 3.17 dB for the combination between μ-law companding and DCT, DST, DHT, and DFT, respectively. Also, this approach is evaluated with a different companding factor $(\mu) = 2$, 3, and 5 and the results are shown finally in Table A1.

On the other hand, the BER performance for all these precoding techniques is almost the same performance when compared to the conventional ACO-OFDM as shown in Fig. 27.

5.2.3. *PAPR and BER performance for precoding techniques combined with A-law companding*

Figures 28 and 29 show the PAPR and BER performance, respectively for the precoding techniques when combined with A-law companding under ACO-OFDM system with the companding factor (A) equalling 3. The value of $PAPR_0$ at $CCDF = 10^{-2}$ equals 9.70, 10.88, 11.57, and 13.96 dB for DCT, DST, DHT, and DFT combined with A-law companding, respectively. Consequently, the PAPR reduction value when compared to the conventional ACO-OFDM system is 6.40, 5.22, 4.53, and 2.14 dB for the combination between A-law companding and DCT, DST, DHT, and DFT, respectively. Also, this approach is evaluated with a different companding factor (A) = 2, 3, and 5 and the results are shown finally in Table A1.

On the other hand, the BER performance for all these precoding techniques is almost the same performance when compared to the conventional ACO-OFDM as shown in Fig. 29.

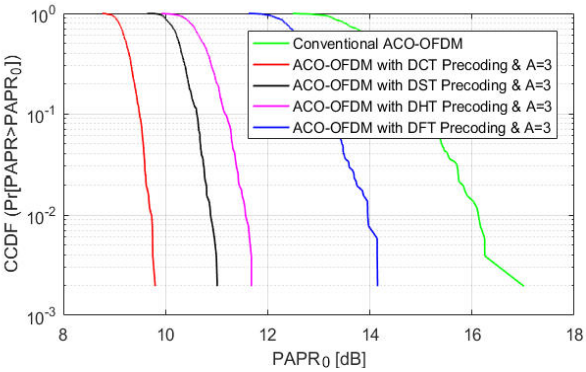

Fig. 28. PAPR comparison between precoding techniques combined with A-law companding for ACO-OFDM system.

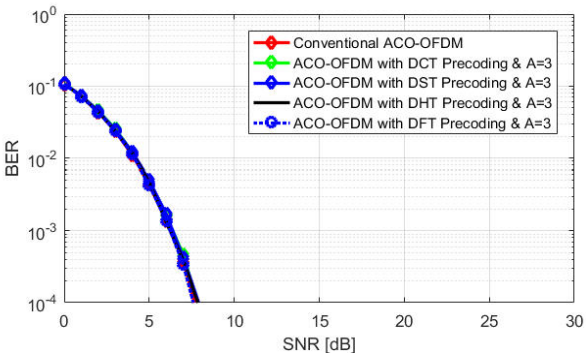

Fig. 29. BER comparison between precoding techniques combined with A-law companding for ACO-OFDM system.

5.2.4. *PAPR and BER performance for spreading techniques*

This section also shows the results of PAPR and BER performance for DCT, DST, DFT, and DHT-spreading techniques under ACO-OFDM system. As shown in Fig. 30, at $CCDF = 10^{-2}$, the spreading techniques of DCT, DST, DHT, and DFT reduce the PAPR to a value of nearly 13.18, 13.33, 14.19, and 12.92 dB, respectively. Consequently, the PAPR reduction value is 2.92, 2.77, 1.91, and 3.18 dB for DCT, DST, DHT, and DFT, respectively when compared to the conventional ACO-OFDM system.

On the other hand, the BER performance for all these spreading techniques is almost the same and the value of E_b/N_0 is 3.85 dB at $BER = 10^{-3}$ which means that the spreading techniques has a gain of 2.55 dB compared to the conventional ACO-OFDM as shown in Fig. 31.

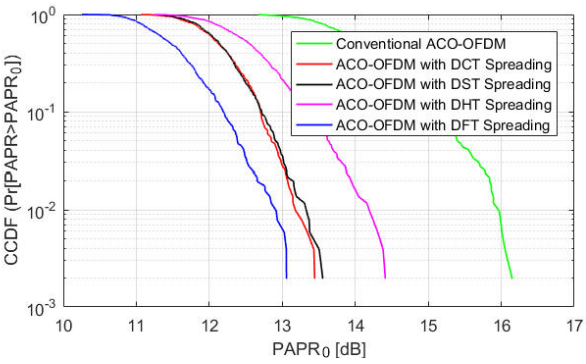

Fig. 30. PAPR comparison between DCT, DST, DHT, and DFT spreading techniques for ACO-OFDM system.

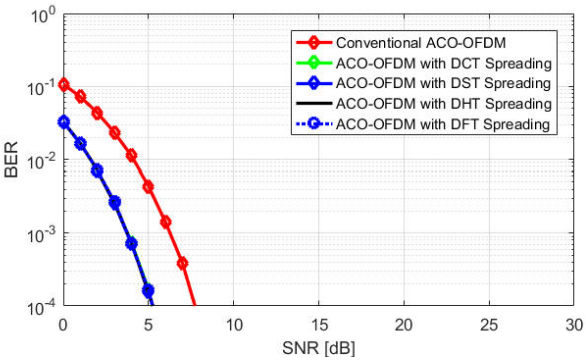

Fig. 31. BER comparison between DCT, DST, DHT, and DFT-spreading techniques for ACO-OFDM system.

5.2.5. *PAPR and BER performance for spreading techniques combined with μ-law companding*

Figures 32 and 33 show the PAPR and BER performance, respectively for the spreading techniques when combined with μ-law companding under ACO-OFDM system with the companding factor (μ) equalling 3. The value of $PAPR_0$ at $CCDF = 10^{-2}$ equals 10.4, 10.4, 11.11, and 10.04 dB for DCT, DST, DHT, and DFT combined with μ-law companding, respectively. Consequently, the PAPR reduction value when compared to the conventional ACO-OFDM system is 5.7, 5.7, 4.99, and 6.06 dB for the combination between μ-law companding and DCT, DST, DHT, and DFT, respectively. Also, this approach is evaluated with a different companding factor (μ) = 2, 3, and 5 and the results are shown finally in Table A1.

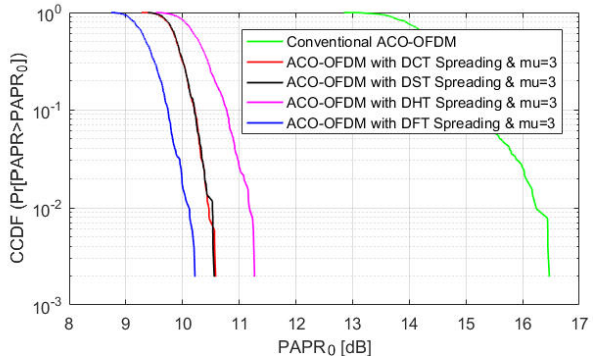

Fig. 32. PAPR comparison between spreading techniques combined with μ-law companding for ACO-OFDM system.

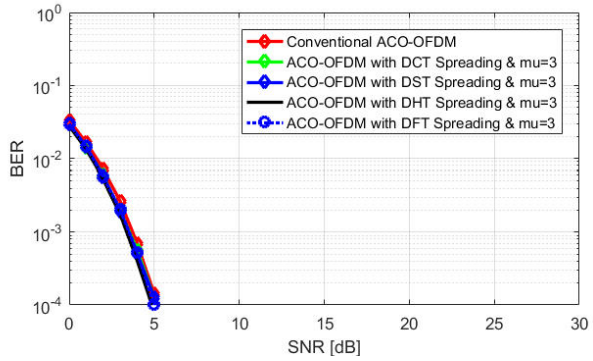

Fig. 33. BER comparison between spreading techniques combined with μ-law companding for ACO-OFDM system.

On the other hand, the BER performance for all these spreading techniques when combined with μ-law companding is almost the same and the value of E_b/N_0 is around 3.60 dB at $BER = 10^{-3}$ which means that the spreading techniques have a gain of 2.80 dB compared to the conventional ACO-OFDM as shown in Fig. 33.

5.2.6. *PAPR and BER performance for spreading techniques combined with A-law companding*

Figures 34 and 35 show the PAPR and BER performance, respectively for the spreading techniques when combined with A-law companding under ACO-OFDM system with a companding factor (A) equalling 3. The value of $PAPR_0$ at $CCDF = 10^{-2}$ equals 10.88, 10.88, 11.58, and 10.51 dB for DCT, DST, DHT, and DFT, combined with A-law companding, respectively. Consequently, the PAPR reduction value when compared to the conventional ACO-OFDM system is 5.22, 5.22, 4.52, and 5.59 dB for the combination between A-law companding and DCT, DST, DHT, and DFT, respectively. Also, this approach is evaluated with a different companding factor (A) = 2, 3 and 5 and the results are shown finally in Table A1.

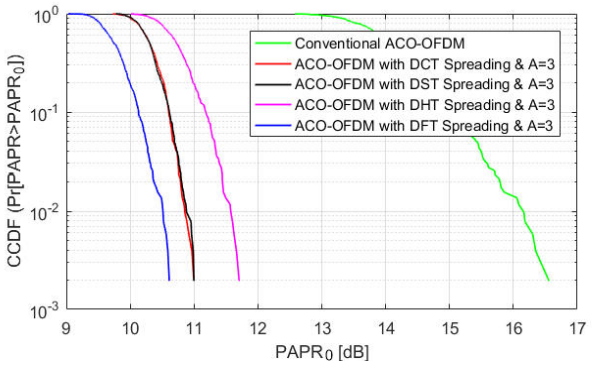

Fig. 34. PAPR comparison between spreading techniques combined with A-law companding for ACO-OFDM system.

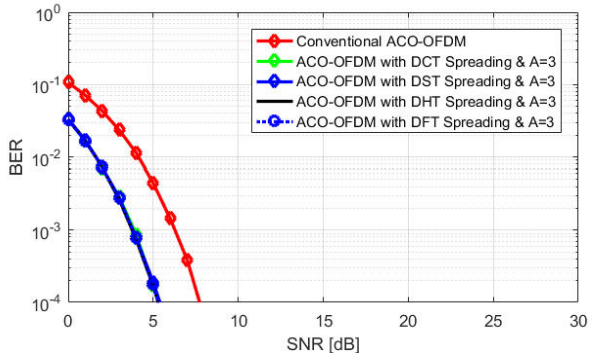

Fig. 35. BER comparison between spreading techniques combined with A-law companding for ACO-OFDM system.

On the other hand, the BER performance for all these spreading techniques when combined with A-law companding is almost the same and the value of E_b/N_0 is around 3.87 dB at $BER = 10^{-3}$ which means that the spreading techniques have a gain of 2.53 dB compared to the conventional ACO-OFDM as shown in Fig. 35.

5.3. *Flip-OFDM*

5.3.1. *PAPR and BER performance for precoding techniques*

This section shows PAPR and BER performance for DCT, DST, DHT, and DFT precoding techniques under Flip-OFDM system. As shown in Fig. 36, at $CCDF = 10^{-2}$, precoding techniques of DCT, DST, DHT, and DFT reduce the PAPR to a value of nearly 13.07, 13.07, 14.16, and 15.69 dB, respectively. Consequently, the PAPR reduction

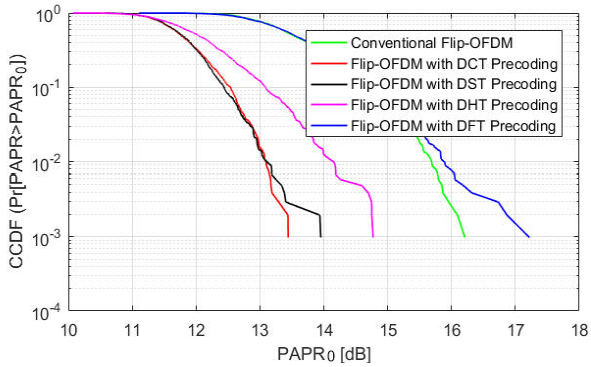

Fig. 36. PAPR comparison between DCT, DST, DHT, and DFT precoding techniques for Flip-OFDM system.

value is 2.83, 2.83, 1.74, and 0.21 dB for DCT, DST, DHT, and DFT, respectively when compared to the conventional Flip-OFDM system.

On the other hand, the BER performance for all these precoding techniques is almost the same performance when compared to the conventional Flip-OFDM as shown in Fig. 37.

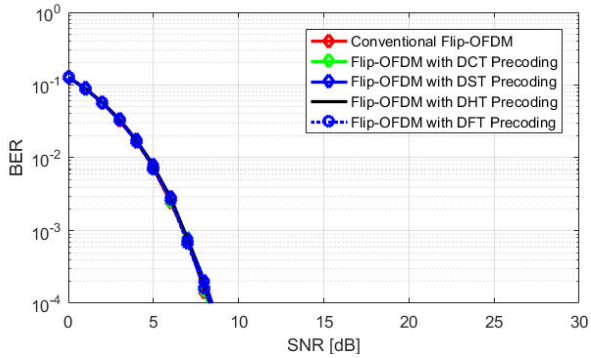

Fig. 37. BER comparison between DCT, DST, DHT, and DFT precoding techniques for Flip-OFDM system.

5.3.2. *PAPR and BER performance for precoding techniques combined with μ-law companding*

Figures 38 and 39 show the PAPR and BER performance, respectively for the precoding techniques when combined with μ-law companding under Flip-OFDM system with a companding factor (μ) equalling 3. The value of $PAPR_0$ at $CCDF = 10^{-2}$ equals 10.24, 10.36, 11.17, and 12.62 dB for DCT, DST, DHT, and DFT combined with

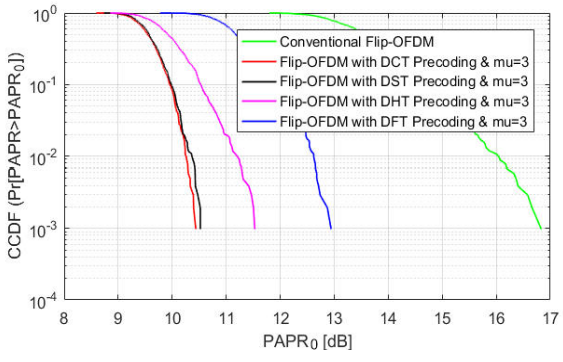

Fig. 38. PAPR comparison between precoding techniques combined with μ-law companding for Flip-OFDM system.

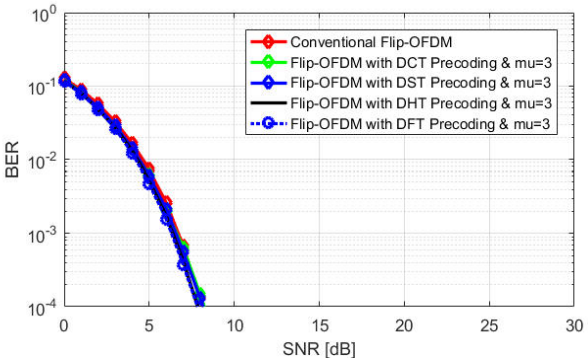

Fig. 39. BER comparison between precoding techniques combined with μ-law companding for Flip-OFDM system.

μ-law companding, respectively. Consequently, the PAPR reduction value when compared to the conventional Flip-OFDM system is 5.66, 5.54, 4.73, and 3.28 dB for the combination between μ-law companding and DCT, DST, DHT, and DFT, respectively. Also, this approach is evaluated with a different companding factor (μ) = 2, 3, and 5 and the results are shown finally in Table A1.

On the other hand, the BER performance for all these precoding techniques is almost the same performance when compared to the conventional Flip-OFDM as shown in Fig. 39.

5.3.3. *PAPR and BER performance for precoding techniques combined with A-law companding*

Figures 40 and 41 show the PAPR and BER performance, respectively for the precoding techniques when combined with A-law companding under Flip-OFDM system with a companding factor (A) equalling 3. The value of $PAPR_0$ at $CCDF = 10^{-2}$ equals 10.07, 10.07, 11.41, and 13.3 dB for DCT, DST, DHT, and DFT combined with A-law companding, respectively. Consequently, the PAPR reduction value when compared to the conventional Flip-OFDM system is 5.83, 5.83, 4.49, and 2.60 dB for the combination between A-law companding and DCT, DST, DHT, and DFT, respectively. Also, this approach is evaluated with a different companding factor (A) = 2, 3, and 5 and the results are shown finally in Table A1.

On the other hand, the BER performance for all these precoding techniques is almost the same performance when compared to the conventional Flip-OFDM as shown in Fig. 41.

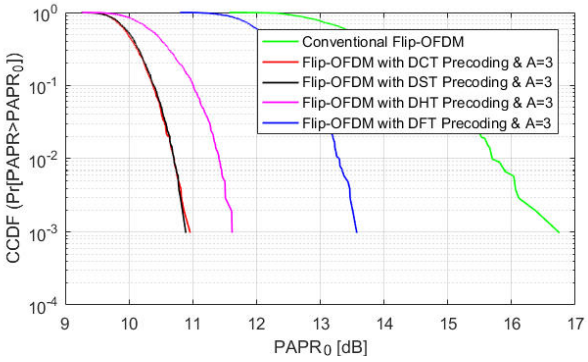

Fig. 40. PAPR comparison between precoding techniques combi-ned with A-law companding for Flip-OFDM system.

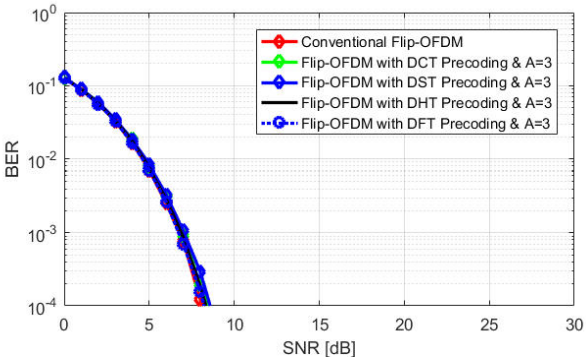

Fig. 41. BER comparison between precoding techniques combined with A-law companding for Flip-OFDM system.

5.3.4. *PAPR and BER performance for spreading techniques*

This section shows the PAPR and BER performance for DCT, DST, DHT, and DFT-spreading techniques under Flip-OFDM system. As shown in Fig. 42, at CCDF = 10^{-2}, spreading techniques of DCT, DST, DHT, and DFT reduce the PAPR to a value of nearly 13.06, 13.06, 14.02, and 12.38 dB, respectively. Consequently, the PAPR reduction value is 2.84, 2.84, 1.88, and 3.52 dB for DCT, DST, DHT, and DFT, respectively when compared to the conventional Flip-OFDM system.

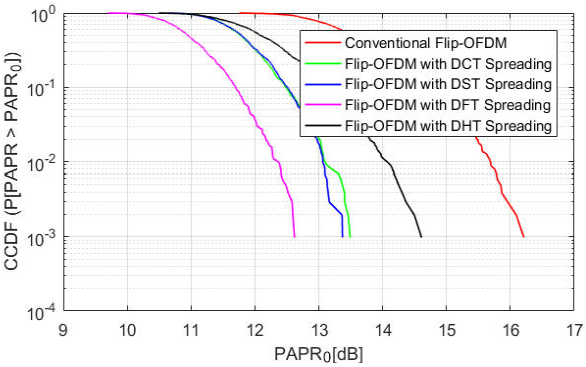

Fig. 42. PAPR comparison between DCT, DST, DHT, and DFT-spreading techniques for Flip-OFDM system.

On the other hand, the BER performance for all these spreading techniques is almost the same and the value of E_b/N_0 is around 3.85 dB at BER = 10^{-3} which means that the spreading techniques have a gain of 2.95 dB compared to the conventional Flip-OFDM as shown in Fig. 43.

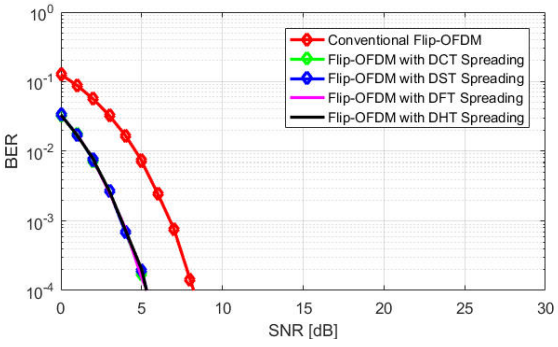

Fig. 43. BER comparison between DCT, DST, DHT, and DFT spreading techniques for Flip-OFDM system.

5.3.5. *PAPR and BER performance for spreading techniques combined with μ-law companding*

Figures 44 and 45 show the PAPR and BER performance, respectively for the spreading techniques when combined with μ-law companding under Flip-OFDM system with the companding factor (μ) equalling 3. The value of $PAPR_0$ at CCDF = 10^{-2} equals 10.38, 10.29, 11.09, and 9.54 dB for DCT, DST, DHT, and DFT combined with μ-law companding, respectively. Consequently, the PAPR reduction value when compared to the conventional Flip-OFDM system is 5.52, 5.61, 4.81, and 6.36 dB for the combination between μ-law companding and DCT, DST, DHT, and DFT, respectively. Also, this approach is evaluated with a different companding factor (μ) = 2, 3, and 5 and the results are shown finally in Table A1.

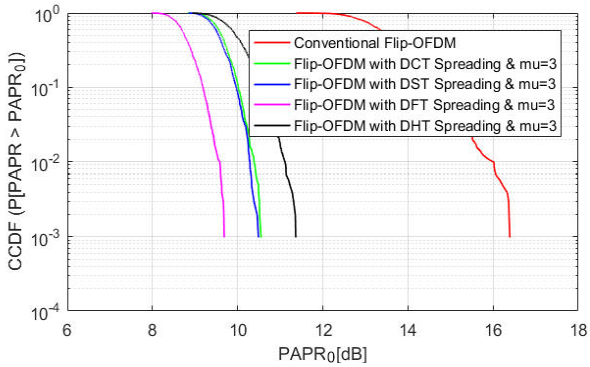

Fig. 44. PAPR comparison between spreading techniques combined with μ-law companding for Flip-OFDM system.

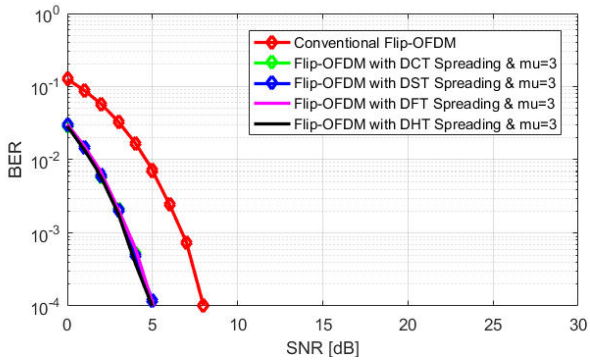

Fig. 45. BER comparison between spreading techniques combined with μ-law companding for Flip-OFDM system.

On the other hand, the BER performance for all these spreading techniques when combined with μ-law companding is almost the same and the value of E_b/N_0 is around 3.68 dB at BER = 10^{-3} which means that the spreading techniques have a gain of 3.12 dB compared to the conventional Flip-OFDM as shown in Fig. 45.

5.3.6. *PAPR and BER performance for spreading techniques combined with A-law companding*

Figures 46 and 47 show the PAPR and BER performance, respectively for the spreading techniques when combined with A-law companding under Flip-OFDM system with a companding factor (A) equalling 3.

The value of $PAPR_0$ at CCDF = 10^{-2} equals 10.89, 10.68, 11.72, and 9.86 dB for DCT, DST, DHT, and DFT combined with A-law companding, respectively. Consequently, the PAPR reduction value when compared to the conventional Flip-OFDM system is 5.01, 5.22, 4.18, and 6.04 dB for the combination between A-law companding and DCT, DST, DHT, and DFT, respectively. Also, this approach is evaluated with a different companding factor (A) = 2, 3, and 5 and the results are shown finally in Table A1.

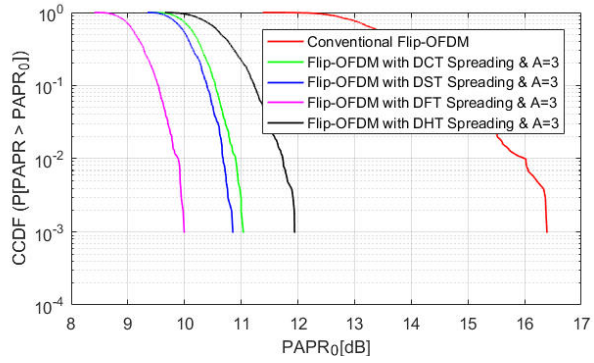

Fig. 46. PAPR comparison between spreading techniques combined with A-law companding for Flip-OFDM system.

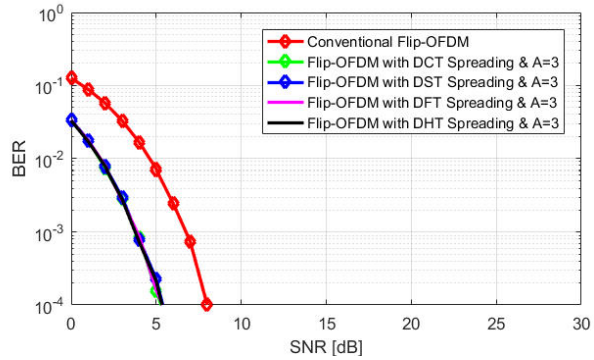

Fig. 47. BER comparison between spreading techniques combined with A-law companding for Flip-OFDM system.

On the other hand, the BER performance for all these spreading techniques when combined with A-law companding is almost the same and the value of E_b/N_0 is around 3.90 dB at BER = 10^{-3} which means that the spreading techniques have a gain of 2.90 dB compared to the conventional Flip-OFDM as shown in Fig. 47.

6. Conclusions

Authors propose several schemes based on a combination of non-linear companding approach and precoding or spreading PAPR reduction techniques. The performance has been evaluated under DCO-OFDM, ACO-OFDM, and Flip-OFDM VLC systems. The comparison between those schemes is performed to extract an effective combination scheme that has a higher PAPR reduction value with the acceptable BER performance. Also, the spectral efficiency and computational complexity of different VLC systems are taken into consideration to find the suitable VLC system merged with a hybrid PAPR reduction scheme that meet the 5G requirements. As mentioned before, in subsection 2.4.1, this DCO-OFDM system has higher spectral efficiency when compared with ACO-OFDM and Flip-OFDM systems at the expense of power efficiency due to the addition of DC-bias. Also, subsection 2.4.2 introduces the fair comparison between these systems in terms of computational complexity. The conclusion of this comparison came in favour of Flip-OFDM and DCO-OFDM. Table A1 shows that the combination between DFT-spreading and μ-law companding at the companding factor ($\mu = 5$) for DCO-OFDM has the highest reduction for PAPR equal to 8.56 dB. However, this reduction came at the expense of BER performance which needs the value of E_b/N_0 to be 14.1 dB. Also, Table A1 indicates that the combination of μ-law companding at the companding factor ($\mu = 5$) and DFT-spreading PAPR reduction technique under Flip-OFDM system achieves the optimum performance of PAPR reduction (PAPR = 8.89 dB) with acceptable BER performance which needs E_b/N_0 to be only 3.84 dB.

References

[1] El-Ganiny, M. Y., Khalaf, A. A. M., Hussein, A. I. & Hamed, H. F. A. A proposed preamble channel estimation scheme for flip FBMC-based indoor VLC systems. *Opto-Electron. Rev*. **30**, e140859 (2022). https://doi.org/10.24425/opelre.2022.140859

[2] Mohammed, N. A., Elnabawy, M. M. & Khalaf, A. A. M. PAPR reduction using a combination between precoding andnon-linear companding techniques foraco-ofdm-based vlc systems. *Opto-Electron. Rev.* **29**, 59–70 (2021). https://doi.org/10.24425/opelre.2021.135829

[3] Yu, T. C. *et al.* Visible light communication system technology review: Devices, architectures, and applications. *Crystals* **11**, 1098 (2021). https://doi.org/10.3390/cryst11091098

[4] Lowery, A. J. Spectrally efficient optical orthogonal frequency division multiplexing. *Phil. Trans. R. Soc. A*. **378**, 20190180 (2020). https://doi.org/10.1098/rsta.2019.0180

[5] Chen, R. *et al.* Visible Light Communication Using DC-Biased Optical Filter Bank Multi-Carrier Modulation. in *2018 Global LIFI Congress (GLC)* 1–6 (2018). https://doi.org/10.23919/GLC.2018.8319094

[6] Sharifi, A. A. PAPR reduction of optical OFDM signals in visible light communications. *ICT Express* **5**, 202–205 (2019). https://doi.org/10.1016/j.icte.2019.01.001

[7] Shaheen, I. A., Zekry, A., Newagy, F. & Ibrahim, R. Performance evaluation of PAPR reduction in FBMC system using nonlinear companding transform. *ICT Express* **5**, 41–46 (2018). https://doi.org/10.1016/j.icte.2018.01.017

[8] Mounir, M., Tarrad, I. F. & Youssef, M. I. Performance evaluation of different precoding matrices for PAPR reduction in OFDM systems. *Internet Technol. Lett.* **1**, e70 (2018). https://doi.org/10.1002/itl2.70

[9] Ahmad, R. & Srivastava, A. PAPR reduction of OFDM signal through DFT precoding and GMSK pulse shaping in indoor VLC. *IEEE Access* **8**, 122092–122103 (2020). https://doi.org/10.1109/ACCESS.2020.3006247

[10] Darwesh, L. & Kopeika, N. Improved performance in the detection of aco-ofdm modulated signals using deep learning modules. *Appl. Sci.* **10**, 8380 (2020). https://doi.org/10.3390/app10238380

[11] Offiong, F. B., Sinanović, S. & Popoola, W. O. Pilot-aided frame synchronization in optical OFDM systems. *Appl. Sci.* **10**, 4034 (2020). https://doi.org/10.3390/app10114034

[12] Freag, H., Hassan, E. S., El-Dolil, S. A. & Dessouky, M. I. New hybrid PAPR reduction techniques for OFDM-based visible light communication systems. *J. Opt. Commun.* **39**, 427–435 (2018). https://doi.org/10.1515/joc-2017-0002

[13] Jiang, T. *et al.* Investigation of DC-Biased optical OFDM with precoding matrix for visible light communications: Theory, simulations, and experiments. *IEEE Photon. J.* **10**, 1–6 (2018). https://doi.org/10.1109/JPHOT.2018.2866952

[14] Wang, Z. & Chen, S. Grouped DFT precoding for PAPR reduction in visible light OFDM systems. *Int. J. Electron. Commun. Comput. Eng*. **6**, 710–713 (2015). https://ijecce.org/administrator/components/com_jresearch/files/publications/IJECCE_3674_Final.pdf

[15] Hesham, H. & Ismail, T. Hybrid NOMA-based ACO-FBMC/OQAM for next-generation indoor optical wireless communications using

LiFi technology. *Opt. Quant. Electron.* **54**, 201 (2022). https://doi.org/10.1007/s11082-022-03559-1
[16] Fernando, N., Hong, Y. & Viterbo, E. Flip-OFDM For Optical Wireless Communications. in *2011 IEEE Inormation Theory Workshop* 5–9 (2011). https://doi.org/10.1109/ITW.2011.6089566
[17] Bahaaelden, M. S., Ortega, B., Perez-Jimenez, R. & Renfors, M. Efficiency analysis of a truncated flip-FBMC in burst optical transmission. *IEEE Access* **9**, 100558–100569 (2021). https://doi.org/10.1109/ACCESS.2021.3096660
[18] Baig, I., Ul Hasan, N., Zghaibeh, M., Khan, I. U. & Saand, A. S. A DST Precoding Based Uplink NOMA Scheme for PAPR Reduction in 5G Wireless Network. in *2017 7th Int. Conference on Modelling Simulation, Applied Optimization* (*ICMSAO*) 1–4 (2017). https://doi.org/10.1109/ICMSAO.2017.7934861
[19] Bardale, R. S. & Yerigiri, V. V. Analysis of DHT-spread ACO-OFDM scheme using binary-psk modulation for PAPR reduction. *Int. J. Electron. Commun. Comput. Eng.* **12**, 22–26 (2017). https://doi.org/10.9790/2834-1206022226
[20] El-Ganiny, M. Y., Khalaf, A. A. M., Hussein, A. I. & Hamed, H. F. A. A preamble based channel estimation methods for FBMC waveform: A comparative study. *Procedia Comput. Sci.* **182**, 63–70 (2021). https://doi.org/10.1016/j.procs.2021.02.009
[21] Saju, S. C. & George, A. J. Comparison of ACO-OFDM and DCO-OFDM in IM / DD Systems. *Int. J. Eng. Res. Technol.* **4**, 1315–1318 (2015). https://www.ijert.org/research/comparison-of-aco-ofdm-and-dco-ofdm-in-imdd-systems-IJERTV4IS041422.pdf
[22] Kumar, M. & Purohit, M. Comparative Study of FLIP-OFDM and ACO-OFDM for Unipolar Communication System. *Int. J. Innov. Sci. Technol.* **1**, 144–148 (2014). https://www.ijiset.com/v1s2/IJISET_V1_I2_25.pdf
[23] Shaheen, I. A., Zekry, A., Newagy, F. & Reem, I. Combined DHT precoding and a-law companding for PAPR reduction in FBMC / OQAM signals. *Int. J. Comput. Academic Res.* **6**, 31–39 (2017). http://www.meacse.org/ijcar/archives/116.pdf
[24] Tsonev, D. & Haas, H. Avoiding Spectral Efficiency Loss in Unipolar OFDM for Optical Wireless Communication. in *2014 IEEE International Conference on Communications (ICC)* 3336–3341 (2014). https://doi/org/10.1109/ICC.2014.6883836
[25] El-Ganiny, M. Y., ElAttar, H. M., Dahab, M. A. A. & Elgarf, T. A. Improved Coding Gain of Clipped OFDM Signal Using Avalanche Effect of AES Block Cipher. in *2017 IEEE Pacific Rim Conference on Communicationm Compututers and Signal Processing (PACRIM)* 1–6 (2017). https://doi.org/10.1109/PACRIM.2017.8121910
[26] Feng, S., Feng, H., Zhou, Y. & Li, B. Low-complexity hybrid optical OFDM with high spectrum efficiency for dimming compatible VLC system. *Appl. Sci.* **9**, 3666 (2019). https://doi.org/10.3390/app9183666
[27] Acolatse, K., Bar-Ness, Y. & Wilson, S. K. Novel techniques of single-carrier frequency-domain equalization for optical wireless communications. *EURASIP J. Adv. Signal Process.* **2011**, 393768 (2011). https://doi.org/10.1155/2011/393768
[28] Pradhan, J., Kappala, V. K., Das, S. & Holey, P. Performance analysis of ACO-OFDM NOMA for VLC communication. *Opt. Quant. Electron.* 54, 531 (2022). https://doi.org/10.1007/s11082-022-03939-7
[29] Ibrahim, A., Prat, J. & Ismail, T. Asymmetrical clipping optical filter bank multi-carrier modulation scheme. *Opt. Quant. Electron.* **53**, (2021). https://doi.org/10.21203/rs.3.rs-248482/v1
[30] Zhou, J. & Zhang, W. Information Rates of Unipolar OFDM Schemes in Gaussian Optical Intensity Channel. in *2017 9th Int. Conference on Wirelss Communication and Signal Processing (WCSP)* 1–7 (2017). https://doi.org/10.1109/WCSP.2017.8170888
[31] Ahmed, F. *et al.* DFT-spread OFDM with quadrature index modulation for practical VLC systems. *Opt. Express* **29**, 33027–33036 (2021). https://doi.org/10.1364/OE.441650
[32] Mhatre, K. & Khot, U. P. Efficient selective mapping PAPR reduction technique. *Procedia Comput. Sci.* **45**, 620–627 (2015). https://doi.org/10.1016/j.procs.2015.03.117
[33] Abd El-Rahman, A. F. *et al.* Companding techniques for SC-FDMA and sensor network applications. *Int. J. Electron. Lett.* **8**, 241–255 (2020). https://doi.org/10.1080/21681724.2019.1600051

Appendix

Table A1.
$PAPR_0$ at CCDF = 10^{-2} and E_b/N_0 at BER = 10^{-3}.

Companding technique	Companding factor	DCT				DST				DHT				DFT			
		CCDF		BER		CCDF		BER		CCDF		BER		CCDF		BER	
		$PAPR_0$	PAPR reduction	E_b/N_0	E_b/N_0 difference	$PAPR_0$	PAPR reduction	E_b/N_0	E_b/N_0 difference	$PAPR_0$	PAPR reduction	E_b/N_0	E_b/N_0 difference	$PAPR_0$	PAPR reduction	E_b/N_0	E_b/N_0 difference
DCO-OFDM (combination between precoding techniques and companding) where conventional DCO-OFDM has $PAPR_0$ = 15.72 dB and E_b/N_0 = 11.82 dB																	
μ-Law	2	10.65	5.07	12.1	0.28	10.65	5.07	12.1	0.28	11.35	4.37	11.9	0.08	12.92	2.8	17.6	5.78
	3	10.14	5.58	12.7	0.88	10.04	5.68	12.5	0.68	10.74	4.98	12.2	0.38	12.07	3.65	30	18.18
	5	9.03	6.69	13.7	1.88	9.44	6.28	13.6	1.78	9.99	5.73	13.3	1.48	11.04	4.68	High	High
A-Law	2	11.75	3.97	11.90	0.08	11.75	3.97	11.90	0.08	12.81	2.91	11.9	0.08	14.67	2.85	12.7	0.88
	3	10.40	5.32	12.4	0.58	10.40	5.32	12.5	0.68	11.43	4.29	12	0.18	13.25	2.47	16	4.18
	5	9.11	6.61	14.4	2.58	9.18	6.54	13.9	2.08	9.67	6.05	13.5	1.68	11.51	4.21	High	High
DCO-OFDM (combination between spreading techniques and companding) where conventional DCO-OFDM has $PAPR_0$ = 15.72 dB and E_b/N_0 = 11.82 dB																	
μ-Law	2	10.61	5.11	11.9	0.08	10.53	5.19	11.9	0.08	11.63	4.09	11.8	0.02	9.86	5.86	12.4	0.58
	3	10.05	5.67	9.5	2.32	10.05	5.67	9.5	2.32	11.64	4.08	9.15	2.67	9.30	6.42	9.7	2.12
	5	9.25	6.47	13.8	1.98	9.25	6.47	13.4	1.58	10.16	5.56	12.8	0.98	8.56	7.16	14.1	2.28
A-Law	2	11.65	4.07	11.8	0.02	11.74	3.98	11.8	0.02	13.03	2.69	11.8	0.02	10.99	4.73	11.9	0.08
	3	10.65	5.07	9	2.82	10.56	5.16	9.2	2.62	11.23	4.49	8.91	2.91	9.82	5.9	9.10	2.72
	5	9.11	6.61	14.5	2.68	9.2	6.52	13.8	1.98	10.11	5.61	12.9	1.08	8.39	7.33	14.7	2.88

ACO-OFDM (combination between precoding techniques and companding) where conventional ACO-OFDM has $PAPR_0$ = 16.10 dB and E_b/N_0 = 6.40 dB																	
μ-Law	**2**	9.91	6.19	5.9	0.5	10.99	5.11	6	0.4	11.64	4.46	5.9	0.5	13.6	2.5	5.9	0.5
	3	9.44	6.66	6	0.4	10.46	5.64	6	0.4	11.06	5.04	5.8	0.6	12.93	3.17	5.8	0.6
	5	8.87	7.23	6.41	0.01	9.77	6.33	6.38	0.02	10.32	5.78	6	0.4	12.04	4.06	6	0.4
A-Law	**2**	10.76	5.34	6.35	0.05	12.1	4	6.45	0.05	12.91	3.19	6.28	0.12	15.35	0.75	6.35	0.05
	3	9.70	6.4	6.50	0.10	10.88	5.22	6.52	0.12	11.57	4.53	6.30	0.10	13.96	2.14	6.35	0.05
	5	8.61	7.49	7	0.6	9.56	6.54	6.90	0.5	10.11	5.99	6.62	0.22	12.16	3.94	6.37	0.03
ACO-OFDM (combination between spreading techniques and companding) where conventional ACO-OFDM has $PAPR_0$ = 16.10 dB and E_b/N_0 = 6.40 dB																	
μ-Law	**2**	10.93	5.17	3.62	2.78	11.01	5.09	3.59	2.81	11.68	4.42	3.54	2.86	10.57	5.53	3.65	2.75
	3	10.4	5.7	3.65	2.75	10.4	5.7	3.65	2.75	11.11	4.99	3.55	2.85	10.04	6.06	3.62	2.78
	5	9.76	6.34	3.82	2.58	9.76	6.34	3.80	2.6	10.35	5.75	3.63	2.77	9.35	6.75	3.78	2.62
A-Law	**2**	12.06	4.04	3.85	2.55	12.12	3.98	3.83	2.57	12.9	3.2	3.84	2.56	11.82	4.28	3.84	2.56
	3	10.88	5.22	3.92	2.48	10.88	5.22	3.87	2.53	11.58	4.52	3.84	2.56	10.51	5.59	3.87	2.53
	5	9.54	6.56	4.3	2.1	9.54	6.56	4.2	2.2	10.12	5.98	3.98	2.42	9.11	6.99	3.98	2.42
Flip-OFDM (combination between precoding techniques and companding) where conventional Flip-OFDM has $PAPR_0$ = 15.90 dB and E_b/N_0 = 6.80 dB																	
μ-Law	**2**	10.86	5.04	6.59	0.21	10.86	5.04	6.62	0.18	11.64	4.26	6.54	0.26	13.12	2.78	6.41	0.39
	3	10.24	5.66	6.65	0.15	10.36	5.54	6.65	0.15	11.17	4.73	6.55	0.25	12.62	3.28	6.45	0.35
	5	9.59	6.31	6.85	0.05	9.59	6.31	6.94	0.14	10.3	5.6	6.65	0.15	11.77	4.13	6.50	0.3
A-Law	**2**	11.89	4.01	6.87	0.07	12.02	3.88	6.97	0.17	12.77	3.13	6.90	0.1	14.88	1.02	6.81	0.01
	3	10.07	5.83	6.92	0.12	10.07	5.83	6.87	0.07	11.41	4.49	6.87	0.07	13.3	2.60	6.80	0
	5	9.52	6.38	7.5	0.7	9.68	6.22	7.3	0.5	10.08	5.82	7.2	0.4	11.87	4.03	6.90	0.1
Flip-OFDM (combination between spreading techniques and companding) where conventional Flip-OFDM has $PAPR_0$ = 15.90 dB and Eb/N_0 = 6.80 dB																	
μ-Law	**2**	10.81	5.09	3.60	3.2	10.82	5.08	3.60	3.2	10.66	5.24	3.57	3.23	10.1	5.8	3.60	3.2
	3	10.38	5.52	3.68	3.12	10.29	5.61	3.65	3.15	11.09	4.81	3.72	3.08	9.54	6.36	3.55	3.25
	5	9.69	6.21	3.80	3	9.60	6.3	3.84	2.96	10.34	5.56	3.65	3.15	8.89	7.01	3.84	2.96
A-Law	**2**	12.07	3.83	3.85	2.95	11.86	4.04	3.83	2.97	13.05	2.85	3.85	2.95	11.13	4.77	3.87	2.93
	3	10.89	5.01	3.90	2.90	10.68	5.22	3.90	2.90	11.72	4.18	3.92	2.88	9.86	6.04	3.85	2.95
	5	9.52	6.38	4.2	2.6	9.39	6.51	4.3	2.5	10.21	5.69	4.15	2.65	8.62	7.28	4.2	2.6